Journal of Quality Measurement and Analysis *JQMA* 20(1) 2024, 81-101
e-ISSN: 2600-8602 *http://www.ukm.my/jqma*
https://doi.org/10.17576/jqma.2001.2024.07

BOUNDARY LAYER FLOW AND HEAT TRANSFER OF CARBON NANOTUBES OVER A MOVING SURFACE IN PRESENCE OF HYDROMAGNETIC

(Aliran Lapisan Sempadan dan Pemindahan Haba dalam Karbon Nanotiub Terhadap Permukaan yang Bergerak dengan Kehadiran Hidromagnet)

AINA ANISAH AHMAD SIDIN & NORFIFAH BACHOK*

ABSTRACT

The aim of this study is to investigate and analyze the influence of hydromagnetic forces on the boundary layer flow and heat transfer of carbon nanotubes over a moving surface. Both types of carbon nanotubes such as single-wall carbon nanotubes and multi-wall carbon nanotubes are considered in this research with two types of base fluid, namely water and kerosene. The governing nonlinear partial differential equations are transformed into a nonlinear ordinary differential equations by using similarity transformations then solved numerically by implementing bvp4c package in MATLAB software. The results obtained were represented in table and graphically illustrated with different values of the moving parameter, magnetic parameter, and carbon nanotubes volume fraction parameter. Additionally, the graphs included in this research are skin friction coefficients and local Nusselt number besides the velocity profile and temperature profile. The results proved that duality solutions exist when the plate and the free stream move in opposite directions. Moreover, the availability of magnetic parameter causes the boundary layer thickness to become thinner and increase the heat transfer.

Keywords: nanofluid; carbon nanotubes; moving plate; hydromagnetic; dual solution

ABSTRAK

Kajian ini meneroka dan mengkaji kesan hidromagnet dalam aliran lapisan sempadan dan pemindahan haba karbon nanotiub terhadap permukaan yang bergerak. Kedua-dua jenis karbon nanotiub seperti karbon nanotiub berdinding tunggal dan karbon nanotiub dinding pelbagai dipertimbangkan dalam kajian ini dengan dua jenis bendalir asas, iaitu air dan kerosin. Persamaan pembezaan separa tak linear dijelmakan menjadi persamaan pembezaan biasa tak linear dengan menggunakan penjelmaan keserupaan yang kemudian diselesaikan secara berangka dengan melaksanakan pakej bvp4c dalam perisian MATLAB. Keputusan yang diperoleh diwakili dalam jadual dan digambarkan secara grafik dengan nilai berbeza bagi parameter bergerak, parameter magnet, dan parameter pecahan isipadu karbon nanotiub. Selain itu, graf yang disertakan dalam kajian ini ialah pekali geseran kulit dan nombor Nusselt selain profil halaju dan profil suhu. Keputusan membuktikan bahawa penyelesaian dual wujud apabila plat dan aliran bebas bergerak dalam arah bertentangan. Selain itu, kewujudan parameter magnet menyebabkan ketebalan lapisan sempadan menjadi lebih tipis dan meningkatkan pemindahan haba.

Kata kunci: bendalir nano; karbon nanotiub; permukaan yang bergerak; hidromagnet; penyelesaian dual

1. Introduction

Nanofluid arose from the growth of the nanotechnology and its ability to improve the performance of solar devices. Nanofluid can be defined as a fluid that contains nanometer-sized particles suspended in a base fluid, resulting in a colloidal solution of nanoparticles in a base

fluid. Metals, oxides, carbides, or carbon nanotubes are commonly utilised as nanoparticles in nanofluids, whereas water, ethylene glycol, and oil serve as base fluids in Ahmed (2019). Choi and Eastman (1995) initially described nanofluid as a fluid containing nanometer-sized particles known as nanoparticles. In nanofluid, there are two model were introduced. Research on the boundary layer of nanofluids, which includes seven slip mechanisms capable of producing a relative velocity between nanoparticles and the base fluid, was conducted by Buongiorno (2006). However, only thermophoresis and Brownian motion have been efficient in modeling nanofluids. The steady boundary layer flow of a nanofluid past a moving sem-infinite flat plate in a uniform free stream was studied by Bachok *et al.* (2010). By using Keller-box method, nonlinear ordinary differential equations were obtained. Bachok *et al.* (2012) extended the research on Blasius and Sakiadis problems in nanofluids and considering a uniform free stream parallel to a fixed or moving flat plate where they investigated the effects of solid volume fraction parameter φ of the nanofluids on the heat transfer. Carbon nanotubes (CNTs) are exemplary nanoparticles found in nanofluids and can be described as cylindrical molecules composed of rolled-up sheets of single-layer carbon atoms (graphene). Carbon nanotubes (CNTs) can be clasified into 2 types which is it can be single-walled (SWCNT) with a diameter of less than 1 nanometer (nm) or multi-walled (MWCNT) with diameters of more than 100 nm and are made up of multiple concentrically interconnected nanotubes. Their length might range from a few micrometres to millimetres. Aladdin *et al.* (2020) stated that the thermal properties and potential of hybrid nanofluids have sparked significant interest among researchers. These hybrid nanofluids offer improved heat transfer rates compared to nanofluids. Hence, Aladdin *et al.* (2020) examined the notable impacts of suction and a magnetic field on a moving plate coated with a hybrid nanofluid comprising water as the base fluid, along with nanoparticles such as Alumina Oxide (Al2O3) and Copper (Cu). Aladdin and Bachok (2020) considered a hybrid nanofluid in their study, specifically focusing on the two-dimensional steady axisymmetric boundary layer. They explored the use of water as the base fluid and two different nanoparticles to form the hybrid nanofluid. The study investigated the behavior of this hybrid nanofluid over a permeable moving plate.

Khan *et al.* (2014) were pioneers in examining the flow and heat transfer characteristics of carbon nanotubes (CNTs) over a flat plate, using both single-wall carbon nanotubes (SWNTs) and multi-wall carbon nanotubes (MWCNTs). The magnetohydrodynamic (MHD) flow and heat transfer from water functionalized carbon nanotubes (CNTs). over a static/moving wedge analysed by Khan *et al.* (2015). They solved the problem by determine the effect of thermal conductivity and viscosity of both single-wall carbon nanotubes (SWNTs) and multi-wall carbon nanotubes (MWCNTs) within a base fluid of similar volume. Therefore, an investigation was carried out on these properties. The problem of Bachok *et al*. (2016) were extended to the flow and heat transfer characteristics of both single-wall and multi-wall carbon nanotubes (CNTs) on a moving plate with slip effect by Anuar *et al.* (2018). This research considered water and kerosene as base fluid. Furthermore, Asshaari *et al.* (2023) investigated the heat and mass transport of nanofluids of carbon nanotubes and water, which were flowing through a moving plate. They utilized the Tiwari and Das nanofluid models, as well as the Buongiorno nanofluid model, to characterize the problem.

Hydromagnetic, also known as magnetohydrodynamics (MHD) or magneto-fluid dynamics, pertains to the study of the magnetic properties and behavior of electrically conducting fluids. Hannes Alfvén is the first person who used the word magnetohydrodynamics in year of 1942 which magnetohydrodynamics stands for magneto- for magnetic field, hydro- for water and dynamics for movement. The effect of magnetic field on the flow and heat transfer past a continuously moving porous plate in a stationary fluid was studied by Chandran *et al.* (1996).

The presence of magnetic field is to control the flow and heat transfer processes in fluids near different types of boundaries. The study conducted by Rajesh Kumar *et al.* (2002) focused on investigating hydromagnetic convection over a vertically moving surface with uniform suction. Rahman and Al-Hatmi (2014) were investigated the hydromagnetic boundary layer flow and heat transfer characteristics of a nanofluid over a nonlinear inclined stretching surface by considering the effect of convective surface condition. They considered three types of nanoparticles namely copper, aluminium oxide and titanium dioxide and having various shapes such as spherical, cylindrical, arbitrary. In addition, they consist of the three different types of basic fluids, such as water, ethylene glycol, and engine oil. The following relevant publications on a moving plate of nanofluids were also discussed by Mabood *et al.* (2015) and Khashi'ie *et al.* (2022).

Thus, this research extended from Anuar *et al.* (2018) and Aladdin *et al.* (2020) to the problem of boundary layer flow and heat transfer of carbon nanotubes over a moving surface by considering M parameter which indicates the presence of hydromagnetic effects. The new effect of hydromagnetic, implemented in this research, has not yet been published by any researchers. Moreover, both types of carbon nanotubes, single-walled CNTs and multi-walled CNTs are use in this research. The primary goal of this research is to identify both the unique and dual solutions. Therefore, by refering to the past research, it is expected to achieve excellent results.

2. Mathematical Formulation

Consider a two-dimensional, steady over a moving surface in a water and kerosene base fluid containing single-wall and multi-wall carbon nanotubes (CNTs) with the presence of hydromagnetic effects as shown in Figure 1. The governing Eqs. $(1) - (3)$ are constructed by following the previous studies (Anuar *et al.* 2018; Aladdin *et al.* 2020):

$$\frac{\partial u}{\partial x}+\frac{\partial v}{\partial y}=0, \tag{1}$$

$$u\frac{\partial u}{\partial x}+v\frac{\partial u}{\partial y}=\frac{\mu_{nf}}{\rho_{nf}}\frac{\partial^2 u}{\partial y^2}-\frac{\sigma_f B^2}{\rho_f}(u-U), \tag{2}$$

$$u\frac{\partial T}{\partial x}+v\frac{\partial T}{\partial y}=\alpha_{nf}\frac{\partial^2 T}{\partial y^2}, \tag{3}$$

subject to the boundary conditions

$$\begin{aligned} &u=U_w, \quad v=0, \quad T=T_w \quad \text{at } y=0,\\ &u\to U_\infty, \quad T\to T_\infty \quad \text{as} \quad y\to\infty, \end{aligned} \tag{4}$$

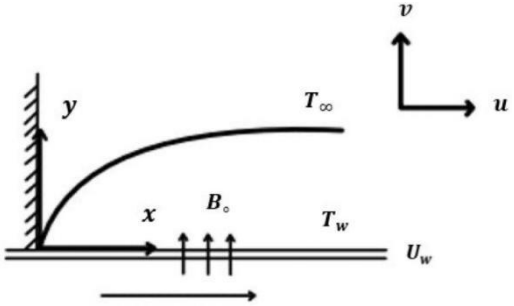

Figure 1: Schematic diagram of the problem

where u and v are the velocity components along the axes x and y, respectively. μ_{nf} is the dynamic viscocity, ρ_{nf} is the density for nanofluid, B is the magnetic field, U is the uniform velocity of the free stream flow, α_{nf} is thermal diffusivity given by

$$\alpha_{nf} = \frac{k_{nf}}{(\rho C_\rho)_{nf}}, \quad \mu_{nf} = \frac{\mu_f}{(1-\varphi)^{2.5}}, \quad \rho_{nf} = (1-\varphi)_{\rho f} + \varphi\rho_{CNT}$$

$$\left(\rho C_\rho\right)_{nf} = (1-\varphi)\left(\rho C_\rho\right)_f + \varphi\left(\rho C_\rho\right)_{CNT}, \tag{5}$$

$$\frac{k_{nf}}{k_f} = \frac{1-\varphi+2\varphi\frac{k_{CNT}}{k_{CNT}-k_f}ln\frac{k_{CNT}+k_f}{2k_f}}{1-\varphi+2\varphi\frac{k_f}{k_{CNT}-k_f}ln\frac{k_{CNT}+k_f}{2k_f}}$$

Here, φ denotes the nanoparticle volume fraction, $(\rho C_\rho)_{nf}$ is the heat capacity of the nanofluid and k is the thermal conductivity which $\frac{k_{nf}}{k_f}$ is determined as given by Anuar *et al.* (2018). Mahapatra *et al.* (2011) stated that the last term in Eq. (2) refers to the *x*-component of the Lorentz force and $B = B_o/\sqrt{2x}$ denotes the magnetic field applied to the fluid flow. Table 1 shows the thermophysical properties for different base fluids.

Table 1: Thermophysical properties of CNTs

Physical Properties	Base Fluids		Nanoparticle	
	Water ($Pr = 6.2$)	Kerosene ($Pr = 21$)	SWCNT	MWCNT
$\rho(kg/m^3)$	997	783	2600	1600
$c_\rho(J/kgK)$	4179	2090	425	796
$k(W/mK)$	0.613	0.145	6600	3000

Also, the similarity transformation from Eq. (6) was taken from Anuar *et al.* (2018).

$$\eta = \left(\frac{U}{v_f x}\right)^{\frac{1}{2}} y, \qquad \psi = \left(v_f x U\right)^{\frac{1}{2}} f(\eta), \qquad \theta(\eta) = \frac{T - T_\infty}{(T_w - T_\infty)}, \quad v_f = \frac{\mu_f}{\rho_f} \tag{6}$$

To solve the boundary layer equation, we introduced a stream function, ψ where $u = \frac{\partial\psi}{\partial y}$ and $v = -\frac{\partial\psi}{\partial x}$ and similarity solution of Eqs. (1)-(3) which identically satisfy Eq. (1). By substituting Eq. (6) into Eqs. (2)-(3), then we derived the reduced equations for momentum and energy, which are presented below:

$$\frac{1}{(1-\varphi)^{2.5}\left[(1-\varphi)+\frac{\varphi\rho_{CNT}}{\rho_f}\right]} f''' + \frac{1}{2} f f'' - M(f'-1) = 0 \tag{7}$$

$$\frac{1}{Pr}\frac{k_{nf}/k_f}{\left[(1-\varphi)+\varphi\left(\rho C_\rho\right)_{CNT}/\left(\rho C_\rho\right)_f\right]}\theta'' + \frac{1}{2} f\theta' = 0 \tag{8}$$

along the BCs,

$$\begin{aligned} &f(0) = 0, \quad f'(0) = \lambda, \quad \theta(0) = 1 \\ &f'(\eta) \to 1 - \lambda, \quad \theta(\eta) \to 0 \ \text{ as } \eta \to \infty \end{aligned} \tag{9}$$

where the primes denotes the differentiation with respect to η . While, Pr is the Prandtl number, λ is the moving parameter and M is the magnetic parameter are defined as:

$$Pr = \upsilon_f/\alpha_f, \qquad U_w = \lambda U, \ \ M = \sigma_f B_o^2/\rho_f U \tag{10}$$

where υ_f is the kinematic viscosity. When $\lambda < 0$ represents the plate and free stream move in opposite direction, while $\lambda > 0$ represents the plate and free stream move in the same direction (Bachok *et al.* 2012).

The physical quantities of interest are skin friction coefficients C_f and local Nusselt number Nu_x, are defined as :

$$C_f = \frac{\tau_w}{\rho_f U^2}, \quad Nu_x = \frac{x q_w}{k_f (T_w - T_\infty)} \tag{11}$$

where τ_w and q_w is the surface shear stress and heat flux are defined as :

$$\tau_w = \mu_{nf} \left(\frac{\partial u}{\partial y}\right)_{y=0}, \qquad q_w = -k_{nf} \left(\frac{\partial T}{\partial y}\right)_{y=0} \tag{12}$$

By substituting Eq. (6) into Eq. (11), we obtain the reduced form of skin friction coefficients and local Nusselt number :

$$\begin{aligned} &C_f Re_x^{-\frac{1}{2}} = \frac{1}{(1-\varphi)^{2.5}} f''(0) \\ &Nu_x Re_x^{-\frac{1}{2}} = -\frac{k_{nf}}{k_f} \theta'(0) \end{aligned} \tag{13}$$

where $Re_x = \frac{U_x}{\upsilon_f}$ is the local Reynolds number.

3. Result and Discussion

The ordinary differential equations (ODEs) of Eqs. (7) - (8) with the boundary conditions in Eq. (9) are solved numerically by implementing bvp4c package in MATLAB software. The dual solutions were obtained by creating an initial guess for the solution of the Eqs. (7) - (8). This is the effective method to solve the problems. Previous researchers, including those cited such as Aladdin *et al.* (2020), Aladdin and Bachok (2020), Anuar *et al.* (2018) and Khashi'ie *et al.* (2022), have achieved successful publication of their research by employing the bvp4c solver for their respective problems.

The numerical findings were obtained by conducting a comparative analysis between the current results and the previously reported research by Anuar *et al.* (2018) in the literature. The relative values of reduced skin friction coefficients $f''(0)$ when $M = 0$ in Table 2 show that the current results and the results of prior investigation in Anuar *et al.* (2018) have a good

correlation. The results were observed to be consistent with the present findings. The thermophysical properties of carbon nanotubes (CNTs) in Khan *et al.* (2014) as a reference as it shown in Table 1 . The main reference utilized in this study is Anuar *et al.* (2018), from which the parameter range is derived. The nanoparticles volume fraction φ is selected within the range of $0 \leq \varphi \leq 0.2$, while the moving parameter λ is varied from 0.2 to 0.4 $(0.2 \leq \lambda \leq 0.4)$. Based on the previous studies, Anuar *et al.* (2018), the existence of unique solutions are validated when $\lambda > 0$ with the plate and free stream moves in the same direction, however, dual solutions are validated when $\lambda_c < \lambda < 0$ with the plate and free stream moves in the opposite direction. On the other hand, magnetic parameter, M is taken from Khashi'ie *et al.* (2022) with values of $M = 0, 0.01, 0.02$. The values taken for the M in this study are slightly smaller than the values of M taken by Aladdin *et al.* (2020). This is because the probability to obtain the duality solution is quite impossible due to the large value of magnetic parameter for $M \geq 0.1$. Meanwhile, Khan *et al.* (2014) was used as a reference for the Prandtl number. The Prandtl number value is different based on the base fluids. Two different types of base fluids used in this study are water and kerosene which respectively uses $Pr = 6.2$ and $Pr = 21$.

Table 2: Comparison $f''(0)$ of water-SWCNT when $M = 0$

φ	λ	Anuar et al. (2018)		Present Result	
		First Solution	Second Solution	First Solution	Second Solution
0	-0.5	0.3978	0.1710	0.3978	0.1710
	-0.4	0.4356	0.0834	0.4356	0.0832
	-0.3	0.4339	0.0367	0.4339	0.0367
	-0.2	0.4124	0.0114	0.4124	0.0114
	-0.1	0.3774	0.0011	0.3774	
	0	0.3321		0.3321	
	0.5	0		0	
	1	-0.4438		-0.4438	
0.1	-0.5	0.3757	0.1615	0.3757	0.1615
	-0.4	0.4114	0.0787	0.4114	0.0782
	-0.3	0.4098	0.0345	0.4098	0.0262
	-0.2	0.3895	0.0107	0.3894	
	-0.1	0.3564	0.0010	0.3564	
	0	0.3136		0.3136	
	0.5	0		0	
	1	-0.4191		-0.4191	
0.2	-0.5	0.3460	0.1488	0.3460	0.1486
	-0.4	0.3789	0.0725	0.3789	0.0699
	-0.3	0.3774	0.0307	0.3774	
	-0.2	0.3587	0.0099	0.3587	
	-0.1	0.3282	0	0.3282	
	0	0.2888		0.2888	
	0.5	0		0	
	1	-0.3861		-0.3860	

Figures 2 and 3 show the graphical results of the effects of φ on reduced skin friction coefficients $f''(0)$ and the effects of φ on reduced heat transfer $-\theta'(0)$ with λ for different φ for water-SWCNTs where the result obtained shows that the existence of unique solution when $\lambda > 0$,while there exist dual solutions when $\lambda_c < \lambda < 0$. In contrast, no solution exists when

$\lambda < \lambda_c$ because boundary layer approximations are physically impossible due to boundary layer separation from the surface. Therefore, from the results obtained in the figures, the increasing values of nanoparticles volume fraction φ cause the skin friction coefficients and heat transfer rate at the surface to decrease. The availability of CNTs makes nanofluids more viscous, which increases their thermal conductivity.

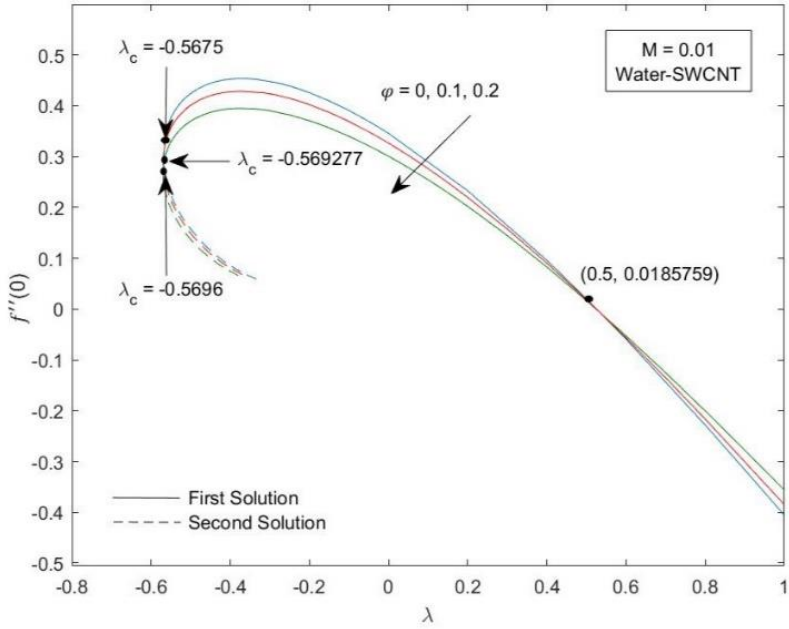

Figure 2: Effect of φ on reduced skin friction coefficients $f''(0)$

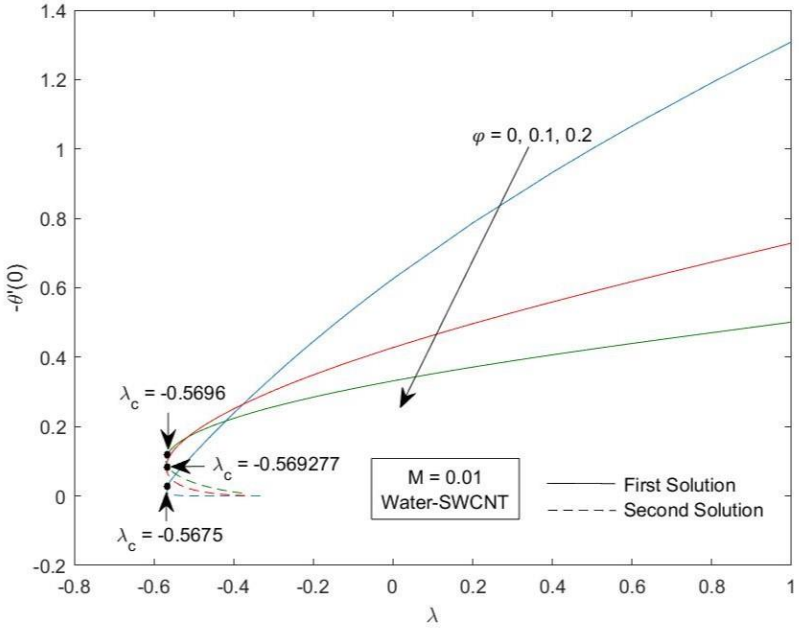

Figure 3: Effect of φ on reduced heat transfer $-\theta'(0)$

Figures 4 and 5 illustrate the results of $f''(0)$ and $-\theta'(0)$ for different values of M in specific range of $M = 0, 0.01, 0.02$ when $\varphi = 0.1$ and $Pr = 6.2$ since this result focus on water-based fluid for single-walled carbon nanotube. According to the observations in Figures 4 and 5, a value of $M = 0$ signifies the absence of any magnetic effect in the fluid. The unique solution exists when $\lambda > 0$ while the duality solutions exists within the range of $\lambda_c < \lambda < 0$ and no solution can be obtained when the value of λ is worth goes above and beyond the critical value, λ_c. From selected value of $M = 0, 0.01, 0.02$, the critical value λ_c achieved $\lambda_c = -0.548248, -0.569279$ and -0.590730 respectively. It clearly demonstrates by adding and increasing the value of *M* influences the reduced skin friction coefficients and reduced heat transfer coefficient to be increased. Indeed, Lorentz force or electromagnetic force which oppose the fluid motion is exerted by the presence of a magnetic field. As a result, heat is produced and the separation of the boundary layer is delayed. The greater the value of M, the greater the delay in thermal boundary layer separation.

The variations of reduced skin friction coefficients f''(0) and reduced heat transfer -θ'(0) by considering both single-walled and multi-walled CNTs with two different base fluid, particularly water and kerosene can be observed in Figures 6 and 7. Observations indicate that for kerosene-SWCNT, the similarity solution exists only when M = 0.01 and λ > λ_c = -0.569128. While, the critical value for λ_c becomes smaller as we use water-SWCNT, λ_c= -0.569279. Critical values for kerosene-MWCNT and water-MWCNT are λ_c= -0.569402 and λ_c= -0.569507 respectively. Hence, it implies that when we used the single-walled CNTs, the reduced skin friction coefficients and heat transfer rate at the surface increases compared to the multi-walled CNTs. Furthermore, as compared to water-based fluid, kerosene-based fluid containing single-walled and multi-walled CNTs produces substantially greater reduced skin friction coefficients and heat transfer rate at the surface.

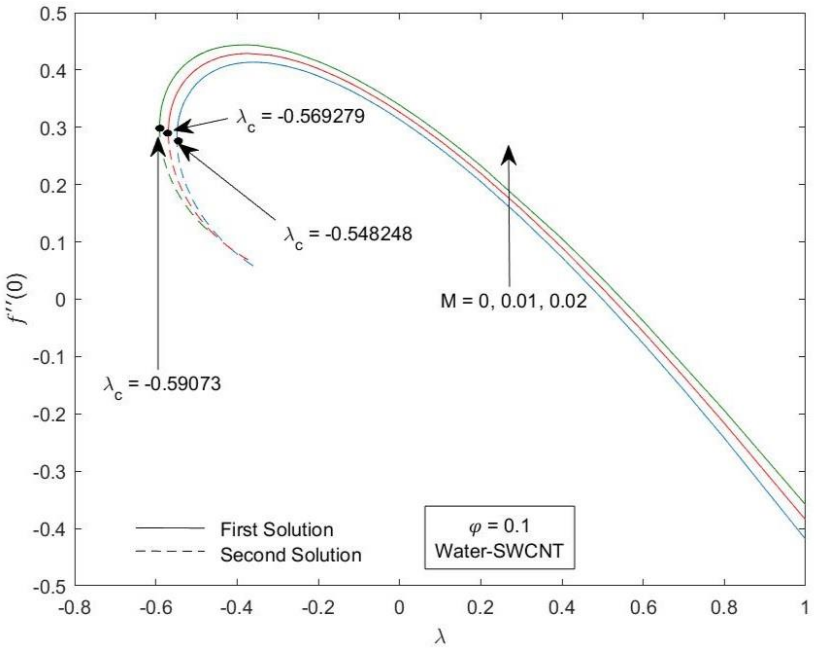

Figure 4: Effect of *M* on reduced skin friction coefficients $f''(0)$

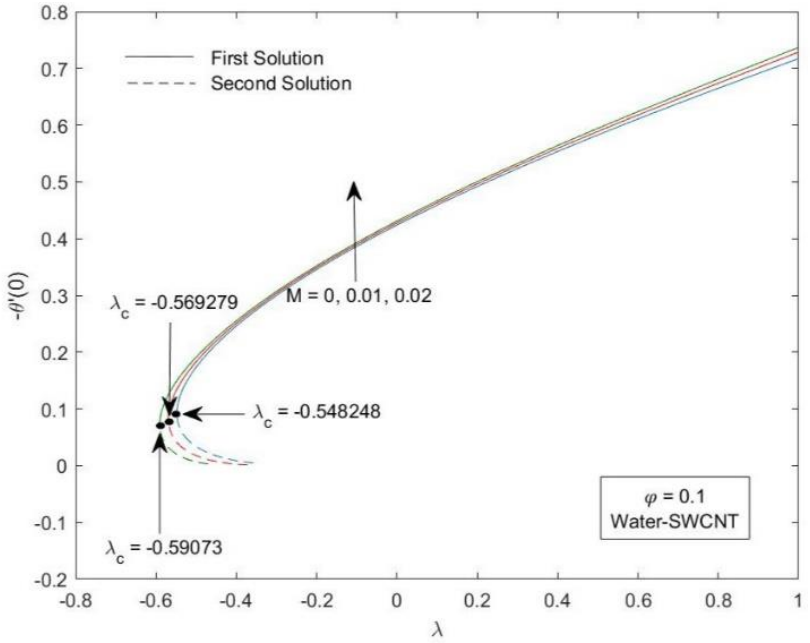

Figure 5: Effect of M on reduced heat transfer $-\theta'(0)$

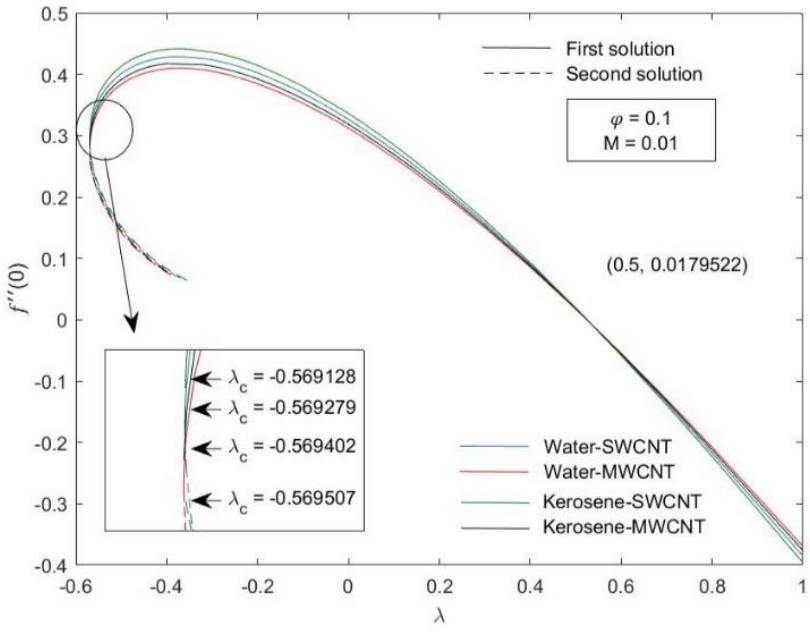

Figure 6: Effect of nanoparticles on reduced skin friction coefficients $f''(0)$

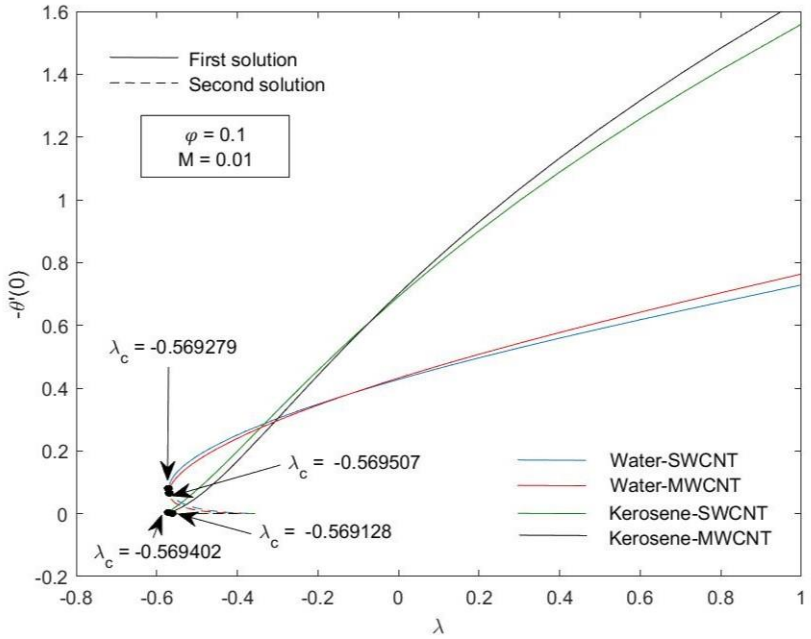

Figure 7: Effect of nanoparticles on reduced heat transfer $-\theta'(0)$

Figures $8-19$ in which local skin friction coefficients and local Nusselt number variations with nanoparticle volume fraction for two types of base fluids are depicted. The graphs in the Figures 8 – 10 depict the graphical results of local skin friction coefficients with various values of *M* with a moving case ($\lambda = 0.2$) for different base fluids (water and kerosene) while taking into account both SWCNTs and MWCNTs. It is clear that when the plate and free stream moves in the same direction, the value of *M* increased, the skin friction coefficients increased as well. Futhermore, the variation of skin friction coefficients with CNTs volume fraction when the plate moves in an aiding flow for both SWCNTs and MWCNTs plotted in Figures $11-13$. It is found that the skin friction coefficients decrease as the moving parameter λ increase in its value $\lambda = 0.2, 0.3, 0.4$. As well as, SWCNTs produced greater skin friction coefficients than MWCNTs which based on Table 1, SWCNTs consist of higher number of density compared to MWCNTs. Lastly, from Figure 13, it is demonstrated that kerosene oil formed higher value of skin friction coefficients more than water.

Figures 14 – 16 depict the effect of M on the variation of local Nusselt number with CNTs volume fraction while taking both SWCNTs and MWCNTs. Besides, these graphs also considering water and kerosene as base fluids same as the previous graphs for local skin friction. The local Nusselt number undoubtedly increase as the magnetic parameter *M* rises. Thus, it is observed that the local Nusselt number for kerosene oil is much higher than the water. The effect of moving parameter λ on local Nusselt number for both types of CNTSs which is SWCNTs and MWCNTs revealed in Figures 17 – 19. Despite of the moving plate moves in the same direction as the free stream, increasing value of moving parameter also influenced the local Nusselt number to be increased for both CNTs. Same as the current graphs for skin friction, we noticed that kerosene base fluid acquired higher local Nusselt number than water base fluid.

The velocity and temperature profiles depicted in Figures 20 – 25 generated from MATLAB are graphically supported and corroborated the numerical solutions and dual solution obtained.

These profiles meet the boundary conditions equation and asymptotically converge with good and accurate results. It is possible to compare the first and second solutions by observing the thickness of boundary layer thickness such that second solution has thicker boundary layer thickness compared to first solution. Figures 20 and 21 illustrate the variations of velocity $f'(\eta)$ and temperature $\theta(\eta)$ profiles respectively. These graphical results focus on the different volume fraction φ for water-SWCNTs. The velocity profiles with increasing CNT volume fraction demonstrate that the profile decrease in the first and second solutions whereas the temperature profile increases when the volume fraction of carbon nanotubes increases.

Figures 22 – 23 represent the variations of velocity $f'(\eta)$ and temperature $\theta(\eta)$ profiles with the effect of M in the water-SWCNTs. The magnetic effects is applied in the range of $M = 0, 0.01,$ and 0.02 in both figures, resulting in $f'(\eta)$ increases significantly in first solution while decreases for second solution. Furthermore, the temperature profile falls as the thermal boundary layer thickness thins for the first solution and increases for the second solution. From both figures, it can be seen that the graphs for second solution are wider for each range of *M* than the graphs for the first solution. Finally, the variations of nanoparticles velocity profiles and temperature profiles with nanoparticle volume fraction of $\varphi = 0.2$ for moving plate case $(\lambda = -0.5)$ are shown in the Figures 24 – 25. In the figures, it discovered that kerosene-SWCNT had a higher velocity and temperature than the others.

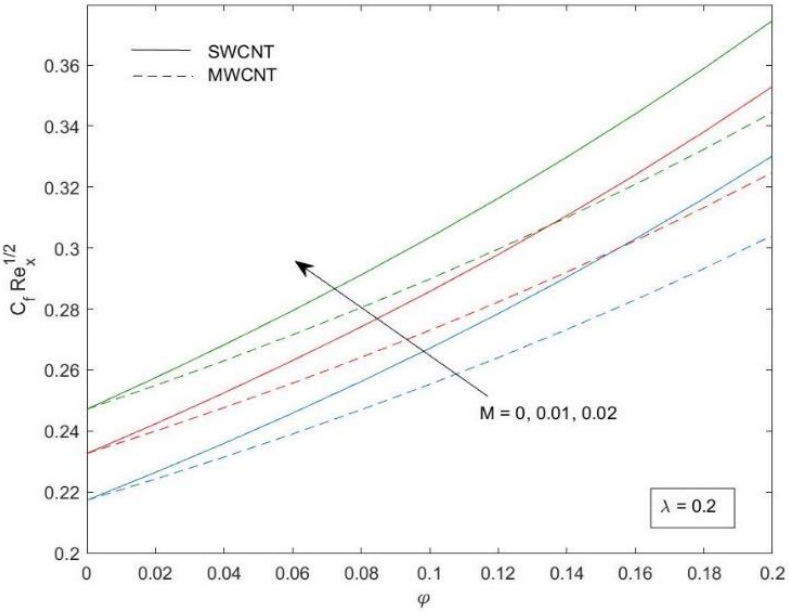

Figure 8: Effect of *M* on skin friction coefficients for water-based fluid

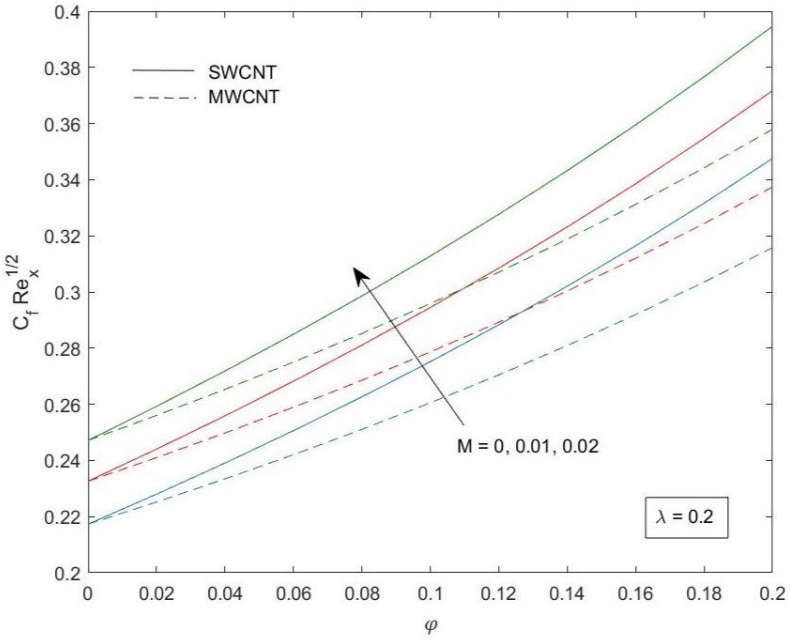

Figure 9: Effect of *M* on skin friction coefficients for kerosene-based fluid

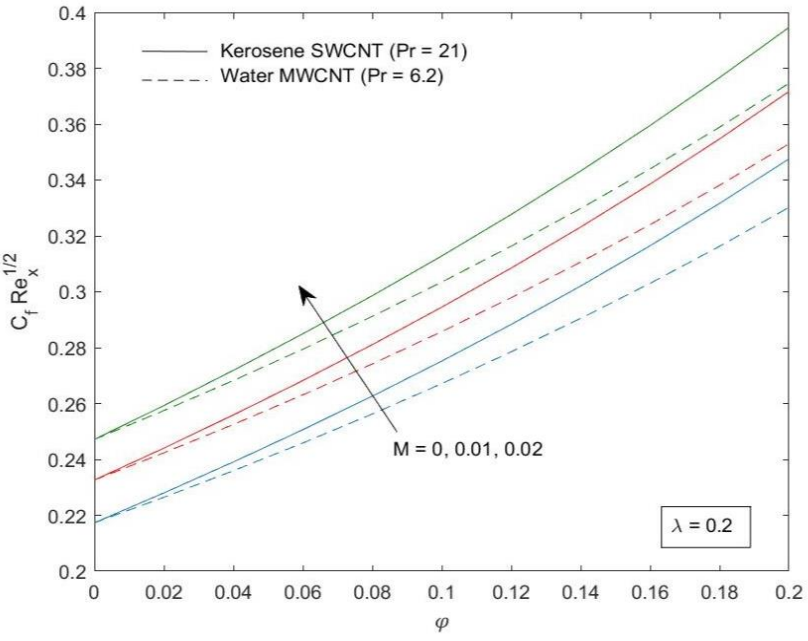

Figure 10: Effect of *M* on skin friction coefficients for water-kerosene based fluid

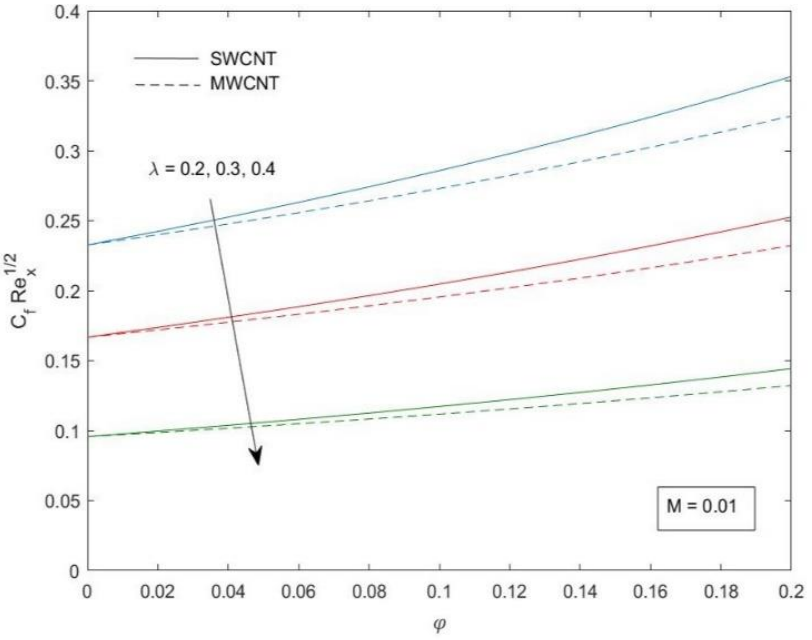

Figure 11: Effect of λ on skin friction coefficients for water-based fluid

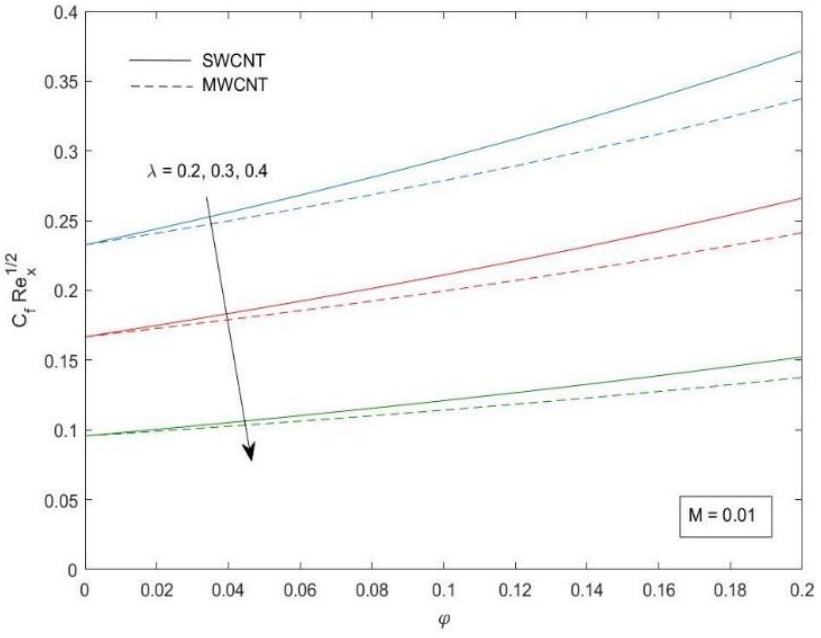

Figure 12: Effect of λ on skin friction coefficients for kerosene-based fluid

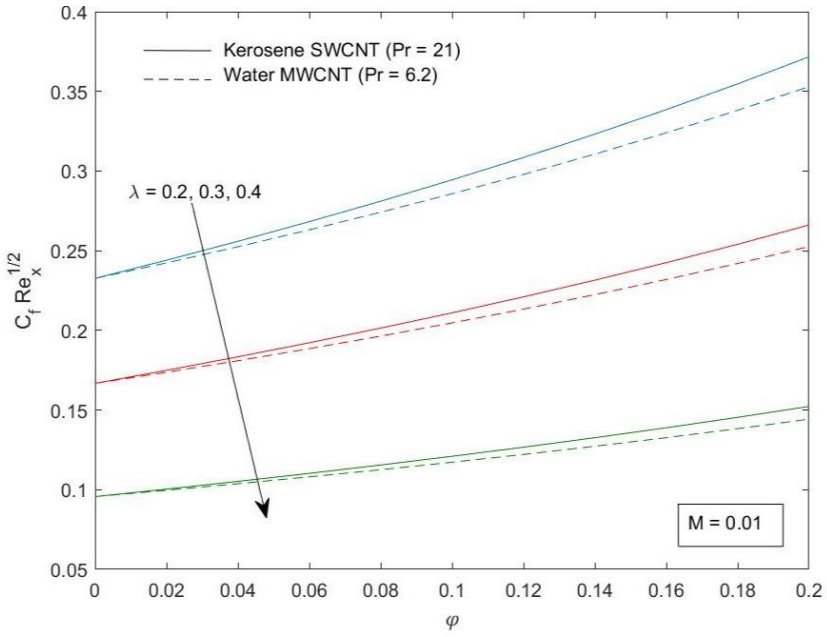

Figure 13: Effect of λ on skin friction coefficients for water-kerosene based fluid

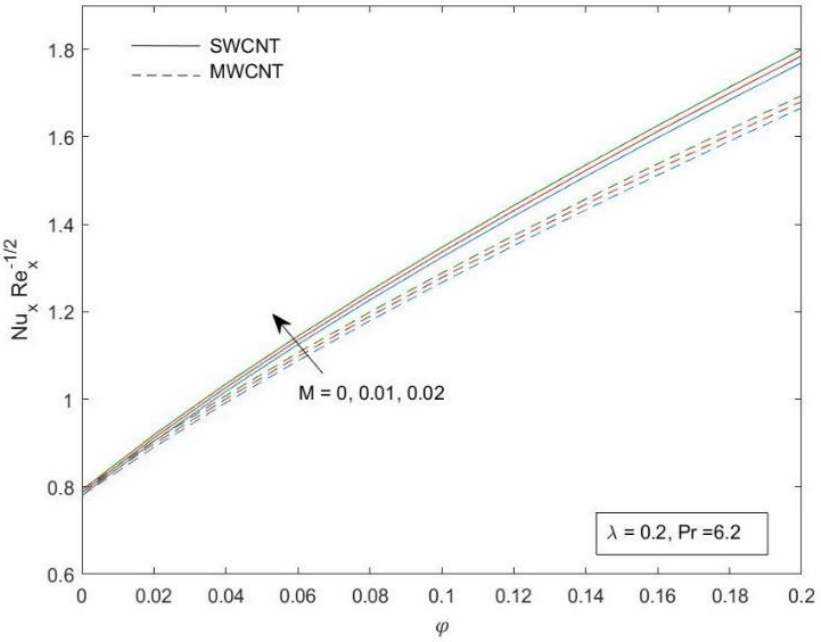

Figure 14: Effect of *M* on local Nusselt number for water-based fluid

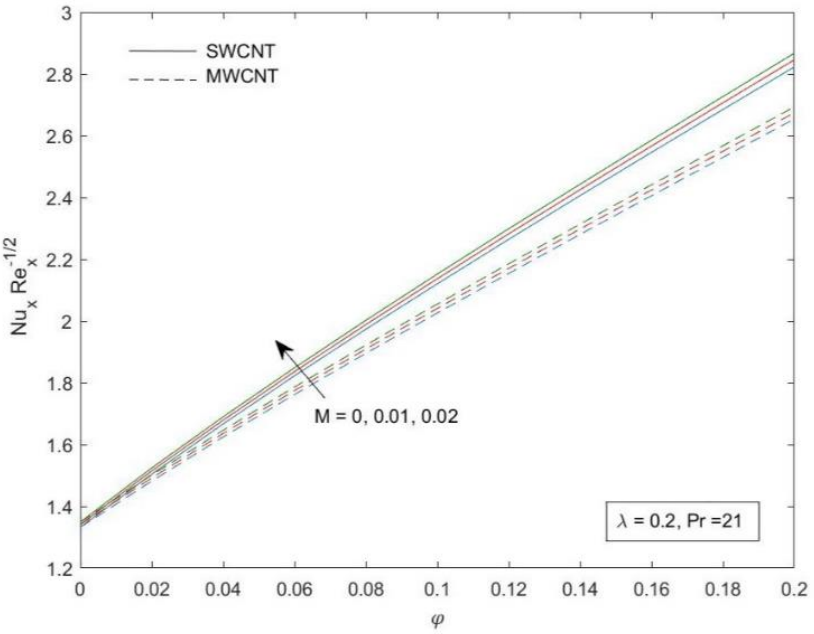

Figure 15: Effect of *M* on local Nusselt number for kerosene-based fluid

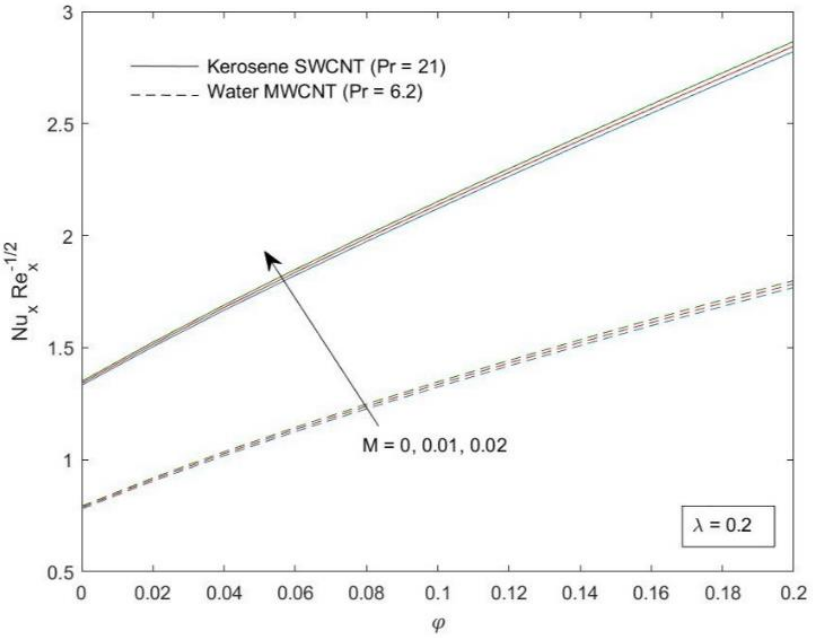

Figure 16: Effect of *M* on local Nusselt number for water-kerosene based fluid

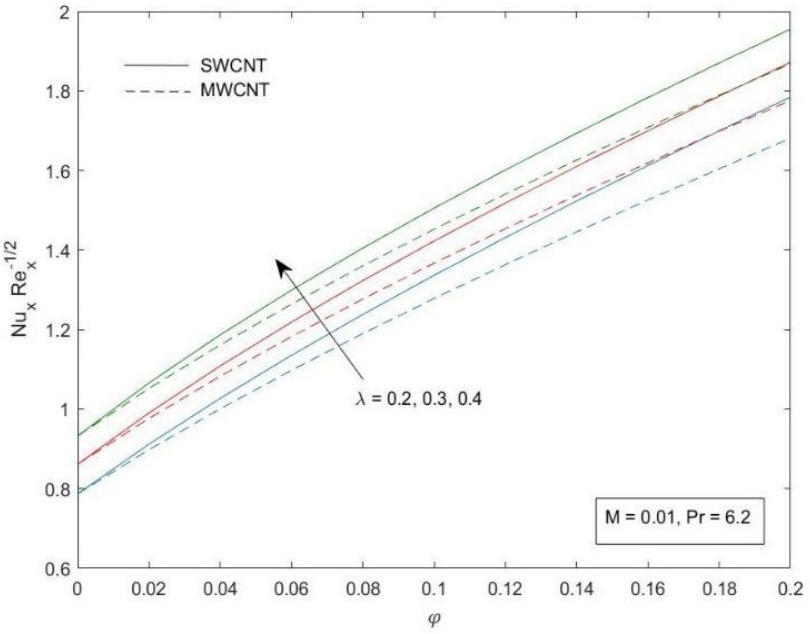

Figure 17: Effect of λ on local Nusselt number for water-based fluid

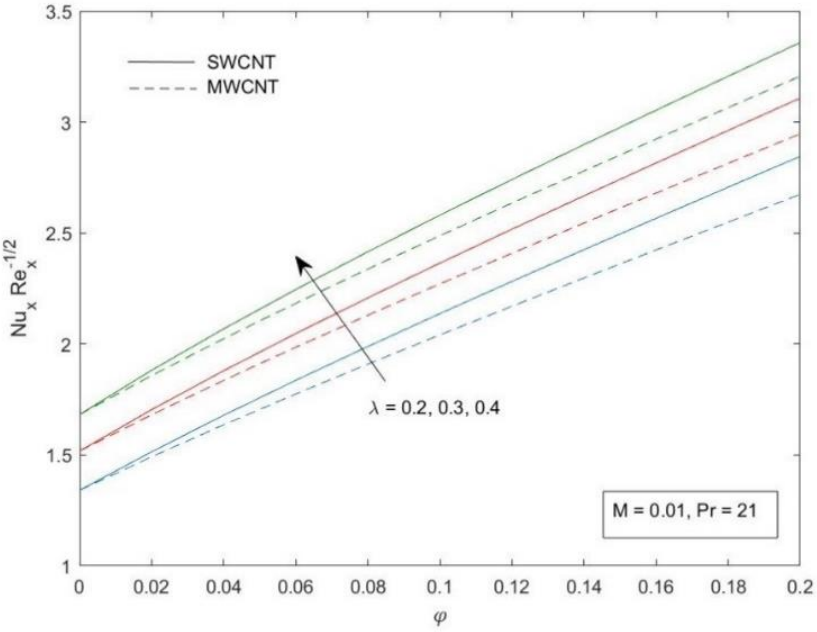

Figure 18: Effect of λ on local Nusselt number for kerosene-based fluid

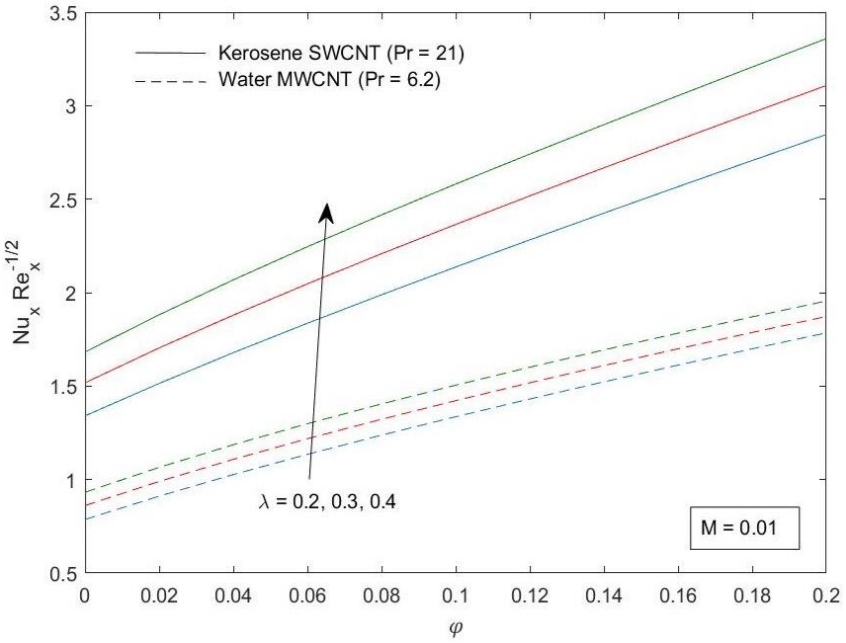

Figure 19: Effect of λ on local Nusselt number for water-kerosene based fluid

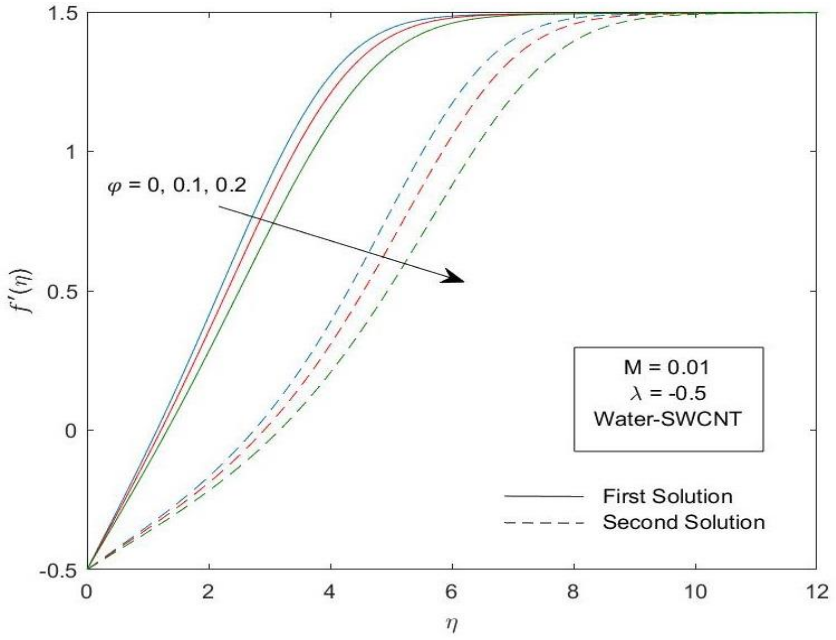

Figure 20: Effect of various φ on velocity profile

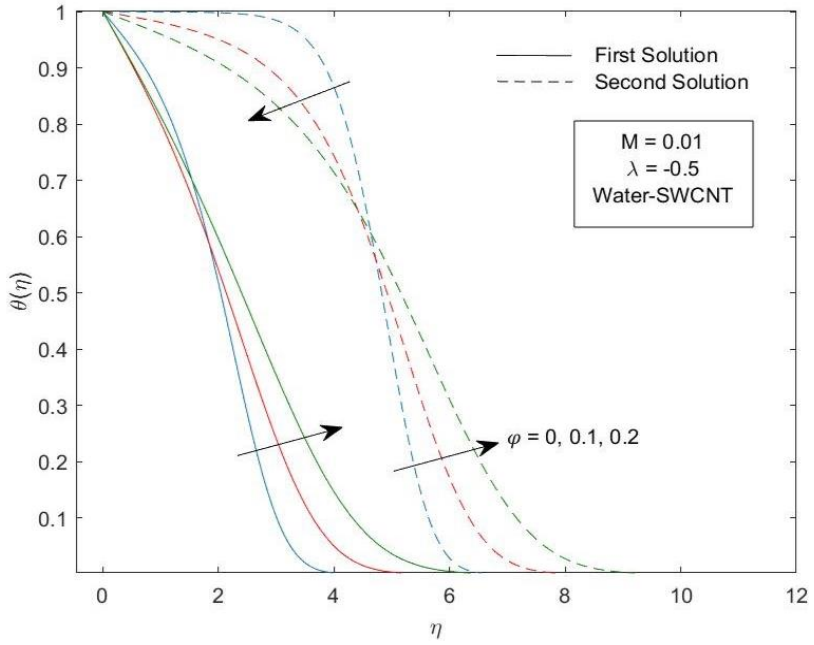

Figure 21: Effect of various φ on temperature profile

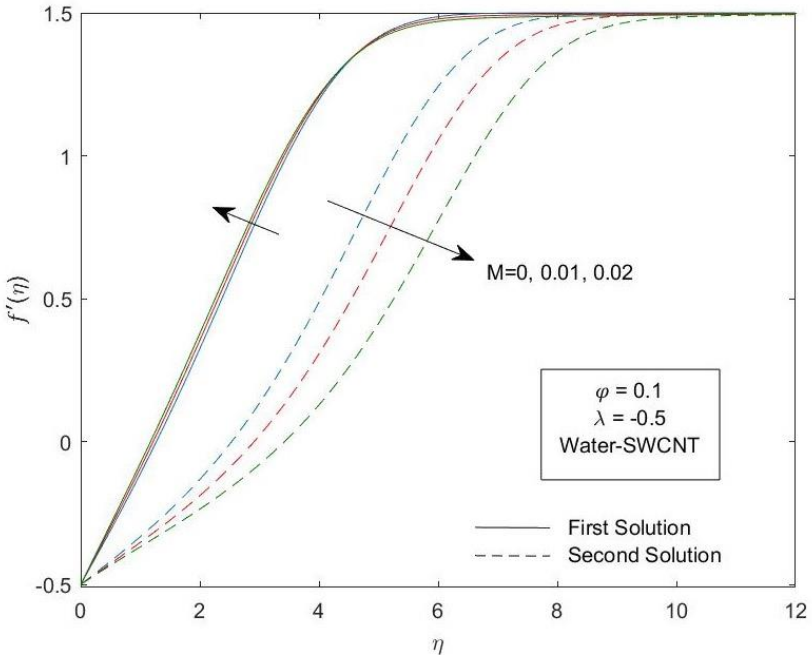

Figure 22: Effect of various *M* on velocity profile

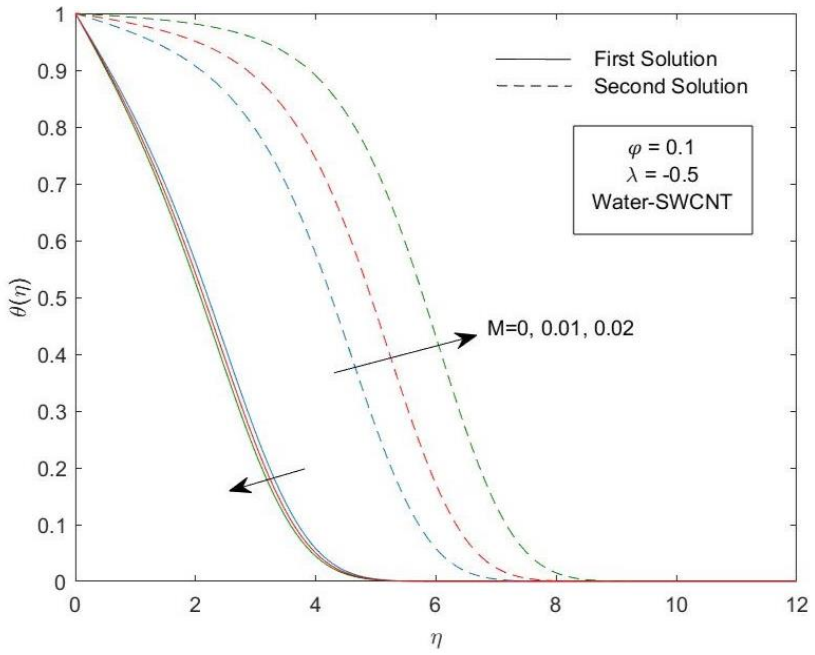

Figure 23: Effect of various *M* on temperature profile

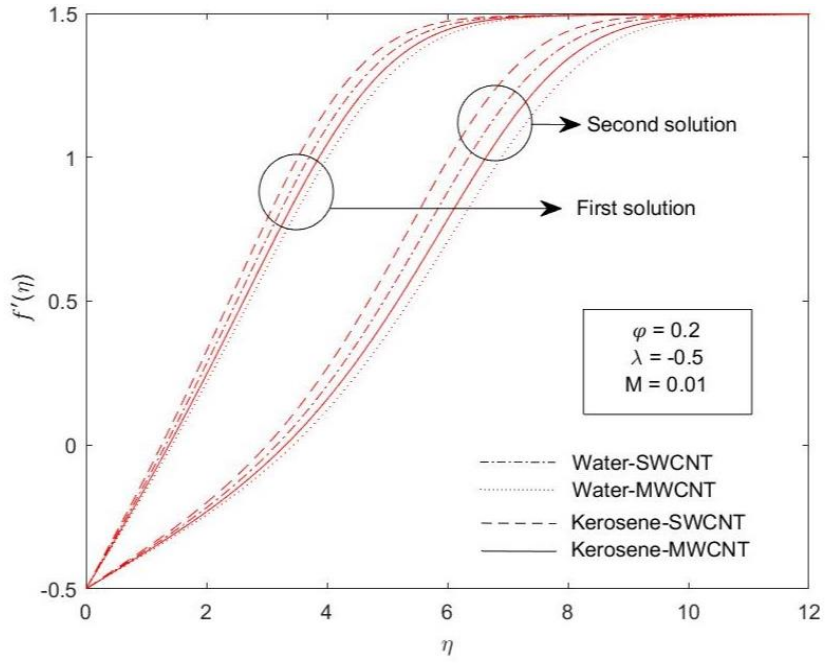

Figure 24: Effect of various nanoparticles on velocity profile

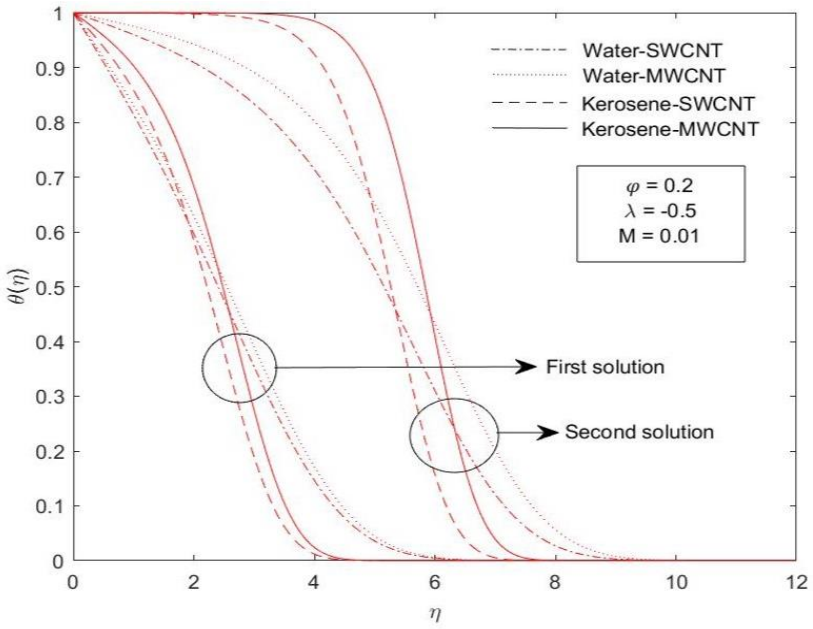

Figure 25: Effect of various nanoparticles on temperature profile

4. Conclusion

The carbon nanotubes over a moving surface in the presence of hydromagnetic effect on the boundary layer flow and heat transfer were examined. Partial differential equations (PDEs) were transformed to ordinary differential equations (ODEs) through the use of similarity transformation. Before utilising MATLAB's bvp4c solver to display the results graphically, the ODEs were numerically solved by creating an initial guess. As a result, the following are the research's findings:

- The solutions are unique when the moving parameter $\lambda > 0$ which represent that the plate moves in the same direction as the free stream while the duality solution exist when $\lambda_c < \lambda < 0$ which represent the plate moves in oppsite direction as the free stream.
- The increment value of magnetic parameter increases the skin friction coefficients and heat transfer as the volume fraction of carbon nanotubes increases.
- As the moving parameter increases, the skin friction coefficients decreases while the heat transfer increases due to an increase in the volume fraction of carbon nanotubes.
- Skin friction coefficients and heat transfer rate are higher in kerosene-based CNTs than in water-based CNTs.
- Single-wall carbon nanotubes (SWCNTs), characterized by their higher density in contrast to multi-wall carbon nanotubes (MWCNTs), exhibit increased effectiveness in terms of skin friction coefficients and heat transfer rate.

References

Ahmed M.S. 2019. Nanofluid: New fluids by nanotechnology. In. *Thermophysical properties of Complex materials*. IntechOpen.

Aladdin N.A.L. & Bachok N. 2020. Boundary layer flow and heat transfer of AL_2O_3-TiO_2/water hybrid nanofluid over a permeable moving plate. *Symmetry* **12**(7): 1064.

Aladdin N.A.L., Bachok N. & Pop I. 2020. Cu-Al_2O_3/water hybrid nanofluid flow over a permeable moving surface in presence of hydromagnetic and suction effects. *Alexandria Engineering Journal* **59**(2): 657–666.

Anuar N.S., Bachok N. & Pop I. 2018. A stability analysis of solutions in boundary layer flow and heat transfer of carbon nanotubes over a moving plate with slip effect. *Energies* **11**(12): 3243.

Asshaari I., Jedi A. & Abdullah S. 2023. Brownian motion and thermophoresis effects in co-flowing carbon nanotubes towards a moving plate. *Results in Physics* **44**: 106165.

Bachok N., Ishak A. & Pop I. 2010. Boundary-layer flow of nanofluids over a moving surface in a flowing fluid. *International Journal of Thermal Sciences* **49**(9): 1663–1668.

Bachok N., Ishak A. & Pop I. 2012. Flow and heat transfer characteristics on a moving plate in a nanofluid. *International Journal of Heat and Mass Transfer* **55**(4): 642–648.

Bachok N., Najib N., Arifin N.M. & Senu N. 2016. Stability of dual solutions in boundary layer flow and heat transfer on a moving plate in a copper-water nanofluid with slip effect. *WSEAS Transactions on Fluid Mechanics* **11**: 151–158.

Buongiorno J. 2006. Convective transport in nanofluids. *Journal of Heat and Mass Transfer* **128**(3): 240-250.

Chandran P., Sacheti N.C. & Singh A. 1996. Hydromagnetic flow and heat transfer past a continuously moving porous boundary. *International Communications in Heat and Mass Transfer* **23**(6): 889–898.

Choi S.U.S & Eastman J.A. 1995. Enhancing thermal conductivity of fluids with nanoparticles. *Proceedings of the ASME International Mechanical Engineering Congress and Exposition*, pp 1-8.

Khan W.A., Khan Z.H. & Rahi M. 2014. Fluid flow and heat transfer of carbon nanotubes along a flat plate with navier slip boundary. *Applied Nanoscience* **4**(5): 633–641.

Khan W.A., Culham R. & Haq R.U. 2015. Heat transfer analysis of mhd water functionalized carbon nanotube flow over a static/moving wedge. *Journal of Nanomaterials* **2015**: 934367.

Khashi'ie N.S., Arifin N.M. & Pop I. 2022. Magnetohydrodynamics (MHD) boundary layer flow of hybrid nanofluid over a moving plate with joule heating. *Alexandria Engineering Journal* **61**(3): 1938–1945.

Mabood F., Khan W.A. & Ismail A.I.M. 2015. MHD boundary layer flow and heat transfer of nanofluids over a nonlinear stretching sheet: a numerical study. *Journal of Magnetism and Magnetic Materials* **374**: 569–576.

Mahapatra T.R., Nandy S.K. & Gupta A.S. 2011. Momentum and heat transfer in mhd stagnation-point flow over a shrinking sheet. *Journal of Applied Mechanics* **78**(2): 021015.

Rahman M.M. & Al-Hatmi M.M. 2014. Hydromagnetic boundary layer flow and heat transfer characteristics of a nanofluid over an inclined stretching surface in the presence of a convective surface: A comprehensive study. *Sultan Qaboos University Journal for Science [SQUJS]* **19**(2): 53–76.

Rajesh Kumar B., Raghuraman D. & Muthucumaraswamy R. 2002. Hydromagnetic flow and heat transfer on a continuously moving vertical surface. *Acta Mechanica* **153**(3): 249–253.

Department of Mathematics and Statistics
Faculty of Science
Universiti Putra Malaysia
43400 UPM Serdang
Selangor DE, MALAYSIA
E-mail: 200678@student.upm.edu.my, norfifah@upm.edu.my[*]

Received: 5 May 2023
Accepted: 18 August 2023

[*]Corresponding author